Results in Physics 43 (2022) 106081

Contents lists available at ScienceDirect

Results in Physics

journal homepage: www.elsevier.com/locate/rinp

Thermosolutal natural convective transport in Casson fluid flow in star corrugated cavity with Inclined magnetic field

Imtiaz Ali Shah [a], S. Bilal [a], Arshad Riaz [b,*], ElSayed M. Tag El-Din [c], M.M. Alqarni [d], Haneen Hamam [e]

[a] Department of Mathematics, AIR University, Sector E-9, Islamabad, Pakistan
[b] Department of Mathematics, Division of Science and Technology, University of Education, Lahore 54770, Pakistan
[c] Faculty of Engineering and Technology, Future University in Egypt New Cairo 11835, Egypt
[d] Department of Mathematics, College of Sciences, King Khalid University, Abha 61413, Saudi Arabia
[e] Mathematics Department, Umm Al-Qura University, Makkah 24382, Saudi Arabia

ARTICLE INFO

Keywords:
Thermal and solutal convection
Casson fluid
Star corrugated cavity
Inclined MHD, FEM

ABSTRACT

Diffusion mechanism generated because of thermal and solutal buoyant forces in star corrugated cavity filled with Casson liquid is envisioned in this study. Magnetic field making angle of inclination with enclosure is also taken into account. Rectangular plate with isothermal and isoconcentration distributions is installed. To measure optimized variation in associated distributions all the extremities of enclosure are kept at cold temperature and zero concentration. Governing equations are modelled by incorporating conservation laws. After then, complexly formulated model equations and their associated boundary constraint are change in dimensionless structure by obliging variables. Numerical simulations are performed by opting finite element based commercial software renowned as COMSOL. Domain is discretized in the form of triangular and rectangular elements by executing hybrid meshing. Afterwards, non-linear solver (PARADISO) is capitalized to handle system of non-linear equations. Mesh independence test is carried out to assure credibility of conducted simulations. Comparison of results with published literature is also displayed. Graphical and tabular representation describing change is associated fields (velocity, temperature and concentration) against wide range of involved parameters. Change in kinetic energy along with average Sherwood and Nusselt number against different magnitudes of Casson parameter is divulged through tables.

Introduction

Diffusion transport mechanism in liquids resulting due to thermal and species concentration changes is denoted as thermosolutal convection. Depending on orientation of gradients existed during the flow in enclosures multiple type of diffusions occurs. Among these thermosolutal convection has received promising applications in diversified fields, e.g. thermal engineering, geophysics and astrophysics. In addition, in geothermal phenomena the role of stratification produced due to variation in intensification of temperature and solutal distributions is highly beneficial in crystal growth, oceanography and management of water reservoirs. Some highly recommendable utilizations related to current topic are encapsulated in [1–11]. Beghein et al. [12] carried out analysis on effectiveness of assisting and opposing solutal buoyancy force on steady state thermosolutal convection in air enclosed in square cavity. Numerical simulations were performed by Gobin and Bennacer [13] to contemplate multicellular flow structure of binary fluid contained in an enclosure with imposition of horizontal thermosolutal differences. Examination about diffusion under joint influence of inertial and thermal/solutal buoyancy forces was divulged by Aimiri et al. [14]. Deposition of nanocomposite on electrodes by varying mass diffusions with static magnetization was delineated by Zhou et al. [15]. A comprehensive analysis on effect of variation in aspect ratio of annular region on heat mass transport in domain was visualized by Chen et al. [16]. Kefayati and his coauthors [1,17–19] performed computational simulations by LBM method to explicate thermal and solutal diffusivity pehnomenon in closed domains with numerous physical aspects. In addition, for the sake of interest of readers and keeping essence of work in mind some related work is provided in refs. [11,20–25].

Matherials possessing elastic characterisitcs and requires specific

* Corresponding author.
E-mail address: arshad-riaz@ue.edu.pk (A. Riaz).

https://doi.org/10.1016/j.rinp.2022.106081
Received 15 August 2022; Received in revised form 10 October 2022; Accepted 31 October 2022
Available online 1 November 2022

threshold of stress for producing deformation is recongnized as viscoelastic liquids. The effectiveness and appliance of these materials are observed in daily life products e.g. Combination of paints with polymers and solver is good use of these materials and obliged in buildings for renovations along with fabrication of complexed surfaces. Other than this viscoelastic materials also characterizes the features of blood and efficiently used in DNA replication process. Packaging of drugs and refinement of curde oil are also the examples which describes employment of these materials. For comprehsensive response of viscoelastic materials against yielding stress at high shearing viscosity formulating mathematical framework was demarcated by Casson [26]. After this an extensive work on Casson fluid with multiple physical aspects are discussed like Rao et al. [27] delineated impact of surface drag force on yielding stress and found that for infinite shear stress at surface the fluid will behave as solid. Bird et al. [28] analyzed rheology of materials with yields by utilizing Casson fluid model and measured driving gradients beyond and below the critical stress. Some research studies descrbing the importance and characteristics of viscoelastic materials by incorporating Casson model is disclosed in refs. [29–33].

Transportation of fluid regimes under the implementation of transverse magnetization make them more potentially more applicable in different governing problems rather in absence. The liquids which polarizes and respond to magnetic field are called as electrically conducting. In addition, these magnetized liquids store extra energy due to polarization and thus employed in numerous engineering systems like reactor frameworking, coolant in reactors, packaging of instruments, growths of crystals, solar panels and so forth. Garandet et al. [34] demonstrated stratified flow of water in rectangular cavity generated by magnetization and buoyant forces. Rudrariah et al. [35] found decrement in momentum and thermal diffusivities of liquid by providing magnetization. Scaling procedure was opted by Hadid et al. [36] to defined dimensionless representation of magnetic strength parameter for description of flow in different physical circumstances. Tagawa and Ozoe [37] delineated convective flow of mettalic liquid in a cube by applying static magnetic field and measure depreciation in momentum and enhancement in thermal field against Hartmann number. Problem formulation for single phase nanofluid flow in wavy cavity for wide range of Hartmann number was adumbrated by Sheremet et al. [38]. Kifayati and his coresearchers [39,40] comprehended changes in convective flow of liquids in different shaped cavities by executing unfiormly palced magnetic source. Latest developments on convective flow of ordinary and nanofluid flow in confined geometries by measuring diffusion with physical prospectives of magnetic field and installement of objects are encapsulated in [41–48].

It is prompted from accessible literature review and analyzing extensive appearance of thermally and solutaly convective diffusion transport in diversified processes this effort is made. Subsequently, so far examination of above said physical features are not interrogated even with viscous liquid. But in this document we have performed advance study by obliging Casson liquid in star enclosure with corrugations and with employment of magnetic field with inclination. So, the prime consent of all author is on to fill this breach. For this purpose a rectangular fin is installed by providing constant heat and mass distributions. Additonally, results are validated by constructing limitized situation for present case study and compared with existed results.

Formualtion of problem

Description statement

A star shaped enclosure with corrugation filled with laminar and incompressible flow of Casson liquid is taken into account. A rectangular fin of unit length by providing constant temperature and concentration distribution is also installed. Fluid density is assumed to be the function temperature and concentration gradients due to which convection in domain is generated. Inclining magnetic field of uniform strength forming angle γ is considered. Graphical visualization of domain is displayed in Fig. 1.

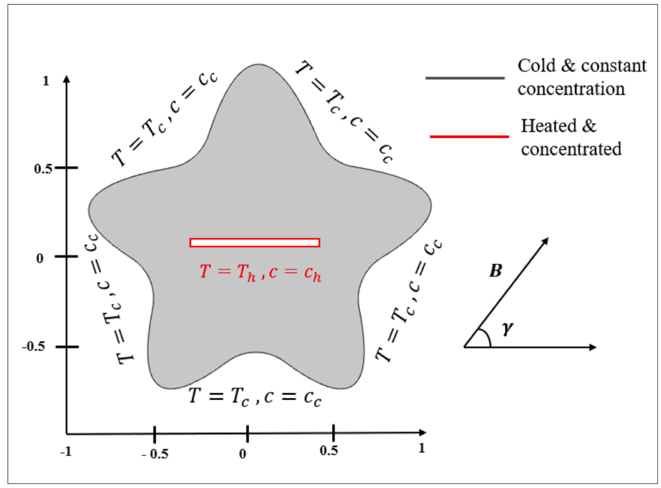

Fig. 1. Graphical description of domain.

Constitutive equations

A Casson fluid model constitutive equation describing the connection between stress and deformation rate is mentioned below [48].

$$\sqrt{\tau^*} = \sqrt{\mu\dot{\gamma}^*} + \sqrt{\tau_0^*}, for \tau^* \geq \tau_0^*,$$

$$\dot{\gamma}^* = 0, for \tau^* \leq \tau_0^* \tag{1}$$

here, τ^* $and \tau_0^*$ represent shearing and yielding stresses.

The govering transport equations for considered problem is as follows [36].

$$\frac{\partial u}{\partial x} + \frac{\partial v}{\partial y} = 0 \tag{2}$$

$$\rho\left(u\frac{\partial u}{\partial x} + v.\frac{\partial u}{\partial y}\right) = -\frac{\partial p}{\partial x} + \mu\left(1+\frac{1}{\beta}\right)\left(\frac{\partial^2 u}{\partial x^2} + \frac{\partial^2 u}{\partial y^2}\right) + \Lambda_x \tag{3}$$

$$\rho\left(u\frac{\partial v}{\partial x} + v\frac{\partial v}{\partial y}\right) = -\frac{\partial p}{\partial y} + \mu\left(1+\frac{1}{\beta}\right)\left(\frac{\partial^2 v}{\partial x^2} + \frac{\partial^2 v}{\partial y^2}\right) + \Lambda_y \tag{4}$$

$$u\frac{\partial T}{\partial x} + v\frac{\partial T}{\partial y} = \alpha_e\left(\frac{\partial^2 T}{\partial x^2} + \frac{\partial^2 T}{\partial y^2}\right) \tag{5}$$

$$u\frac{\partial c}{\partial x} + v\frac{\partial c}{\partial y} = D\left(\frac{\partial^2 c}{\partial x^2} + \frac{\partial^2 c}{\partial y^2}\right) \tag{6}$$

Here, Λ denotes the forcing factor generated due to magnetization.

After utilizing Boussinesq approximation the forcing factor takes following form.

$$\Lambda_x = \sigma B_0^2\left(v sin\gamma cos\gamma - u sin^2\gamma\right) \tag{7}$$

$$\Lambda_y = \sigma B_0^2\left(u sin\gamma cos\gamma - v cos^2\gamma\right) + \rho g[\beta_T(T - T_c) + \beta_c(c - c_c)] \tag{8}$$

Where, β_T and β_c shows the thermosolutal diffusivites, respectively.

Prescribed wall conditions

$$u = 0, v = 0, T = T_h, c = c_h, \left(-\frac{L}{2} \leq x \leq \frac{L}{2}\right), y = 0 \tag{9}$$

$$u = 0, v = 0, T = T_c, c = c_c, \ -L \le x \le L, \ -L \le y \le L \tag{10}$$

Utilization of below mentioned set of variable for conversion into dimensioless resperesentiton.

$$(X^*, Y^*) = \frac{(x,y)}{L}, (U^*, V^*) = \frac{(u,v)L}{\alpha}, P^* = \frac{pL^2}{\rho\alpha^2}, \theta^* = \frac{T - T_c}{T_h - T_c}, C^* = \frac{c - c_c}{c_h - c_c} \tag{11}$$

$$\alpha_e = \frac{k_e}{(\rho c_p)_f}, Ra = \frac{\rho^2 \beta_T g L^3 \Delta T Pr}{\upsilon^2}, Le = \frac{\alpha_e}{\mathrm{D}}, Ha = BL\sqrt{\frac{\mu}{\sigma}}, Pr = \frac{\nu}{\alpha} \tag{12}$$

Non-dimensional visualtization of transport equations is attained below [48].

$$\frac{\partial U^*}{\partial X^*} + \cdot\frac{\partial V^*}{\partial Y^*} = 0 \tag{13}$$

$$\left(U^* \frac{\partial U^*}{\partial X^*} + V^* \cdot \frac{\partial U^*}{\partial Y^*}\right) = -\frac{\partial P^*}{\partial X^*} + Pr\left(1 + \frac{1}{\beta}\cdot\right)\left(\frac{\partial U^*}{\partial X^*}\cdot + \frac{\partial U^*}{\partial Y^*}\right) + \Lambda_{X^*} \tag{14}$$

$$\left(U^* \frac{\partial V^*}{\partial X^*} + V^* \cdot \frac{\partial V^*\cdot}{\partial Y^*}\right) = -\frac{\partial P^*}{\partial Y^*} + Pr\left(1 + \frac{1}{\beta}\cdot\right)\left(\frac{\partial V\cdot^*}{\partial X^*} + \frac{\partial V^*}{\partial Y^*}\right) + \Lambda_{Y^*} \tag{15}$$

$$U^* \frac{\partial \theta^*}{\partial X^*}\cdot + V^* \cdot \frac{\partial \theta^*}{\partial Y^*} = \frac{\cdot\partial^2 \theta^*}{\partial X^{*2}} + \frac{\partial^2 \theta^*}{\partial Y^{*2}} \tag{16}$$

$$U^* \frac{\partial C^*}{\partial X^*} + V^* \frac{\partial C^*\cdot}{\partial Y^*} = \frac{1}{Le}\left(\frac{\partial^2 C^*\cdot}{\partial X^{*2}} + \frac{\partial^2 C^*}{\partial Y^{*2}\cdot}\right) \tag{17}$$

Where,

$$\Lambda_{X^*} = PrHa^2\left(V^* sin\gamma cos\gamma - U^* sin^2\gamma\right) \tag{18}$$

$$\Lambda_{Y^*} = PrHa^2\left(U^* sin\gamma cos\gamma - V^* cos^2\gamma\right) + RaPr(\theta^* + NC^*). \tag{19}$$

Conditions at boundaries of domain in dimensionless structuring is as under.

$$U^* = 0V^* = 0\theta^* = 1C^* = 1\left(-\frac{1}{2} \le X^* \le \frac{1}{2}Y^* = 0\right) \tag{20}$$

$$U^* = 0V^* = 0\theta^* = 0C^* = 0(-1 \le X^* \le 1 - 1 \le X^* \le 1) \tag{21}$$

Corelations defining local and mean heat and mass fluxes are described below.

$$Nu_{local} = -\left.\frac{\partial \theta^*}{\partial n}\right|_{innerwall}, \tag{22}$$

$$Sh_{local} = -\left.\frac{\partial C^*}{\partial n}\right|_{innerwall}, \tag{23}$$

$$Nu_{avg} = \frac{1}{L}\int_L^1 Nu_{local} dL, \tag{24}$$

$$Sh_{avg} = \frac{1}{L}\int_L^1 Sh_{local} dL. \tag{25}$$

Additionally, globally quantified kinetic energy is shown as under.

$$K.E = \frac{1}{2}\int_\Omega \|U\|^2 \, \mathrm{d}\Omega. \tag{26}$$

Compuational scheme

Transport mechanism in fluids in simple confined geometries is easily managed by exact approaches and traditional schemes. But, most of the problems in nature arises is intricate structural designs so previously implemented exact schemes are unable to solve them. For this prupose the analytical approaches are found to be the best for solving these problems. Specifically discussing about the irregular shapes the flow phenomeon is efficiently tackled by versatile method known as finite element method. In this procedure the domain is divided into small portions and variable of interest are computed at element level. Depending on field variables degrees of freedom are computed at different refinement levels as shown in Table 1 and interpolated by utilizing stable element pair. Since, the govering problem discussed here comprises of pressure which is approximated by linear polynomials where as rest of distributions are approximated by quadratic polynomials. Descritization of domain is manifested in Fig. 2 describing hybrid meshing at coarse level with triangular and rectangular elements. Afterwards, system of non-linearized equations are formed and solved by direct solver known as PARADISO. The steps involved in the scheme are presented in Table 1. Convergence criterion adjusted for nonlinear iterations is as follows

Table 1
Meshing at different level of refinements.

Grid	# EL	#DOFs
Extremely coarse	390	2607
Extra coarse	552	3630
Coarser	878	5643
Coarse	1476	9284
Normal	2130	13,189
Fine	3388	20,504
Finer	8092	48,224
Extra fine	20,002	117,161
Extremely fine	27,678	159,379

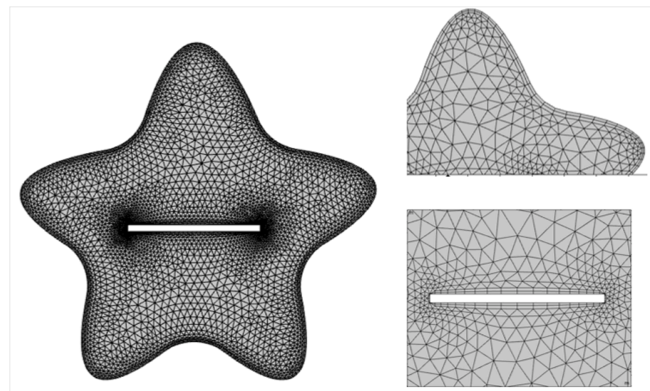

Fig. 2. Element formation in domain at coarser grid.

$$\left|\frac{\chi^{n+1} - \chi^n}{\chi^{n+1}}\right| \langle \, 10^{-6}$$

Where, χ characterizes the general solution component (Fig. 3).

Discretization of equations (Weak Formulation)

Let subspace for $U^*.,V^*.,\theta^*,C^*$ is $W = \left[H^1(\Omega)\right]^3$ be the test subspaces for pressure is $Q = L^2(\Omega)$. The weak form of the governing equation is given as.

$$\int_\Omega \left(U^* \frac{\partial U^*}{\partial X^*} + V^* \cdot \frac{\partial U^*}{\partial Y^*}\right) w d\Omega + \int_\Omega \frac{\partial P^*}{\partial X^*} w d\Omega + Pr\int_\Omega \left[\left(1 + \frac{1}{\beta}\cdot\right)\left(\frac{\partial U^*}{\partial X^*}\cdot + \frac{\partial U^*}{\partial Y^*}\right) + \Lambda_{X^*}\right] w d\Omega = 0, \tag{27}$$

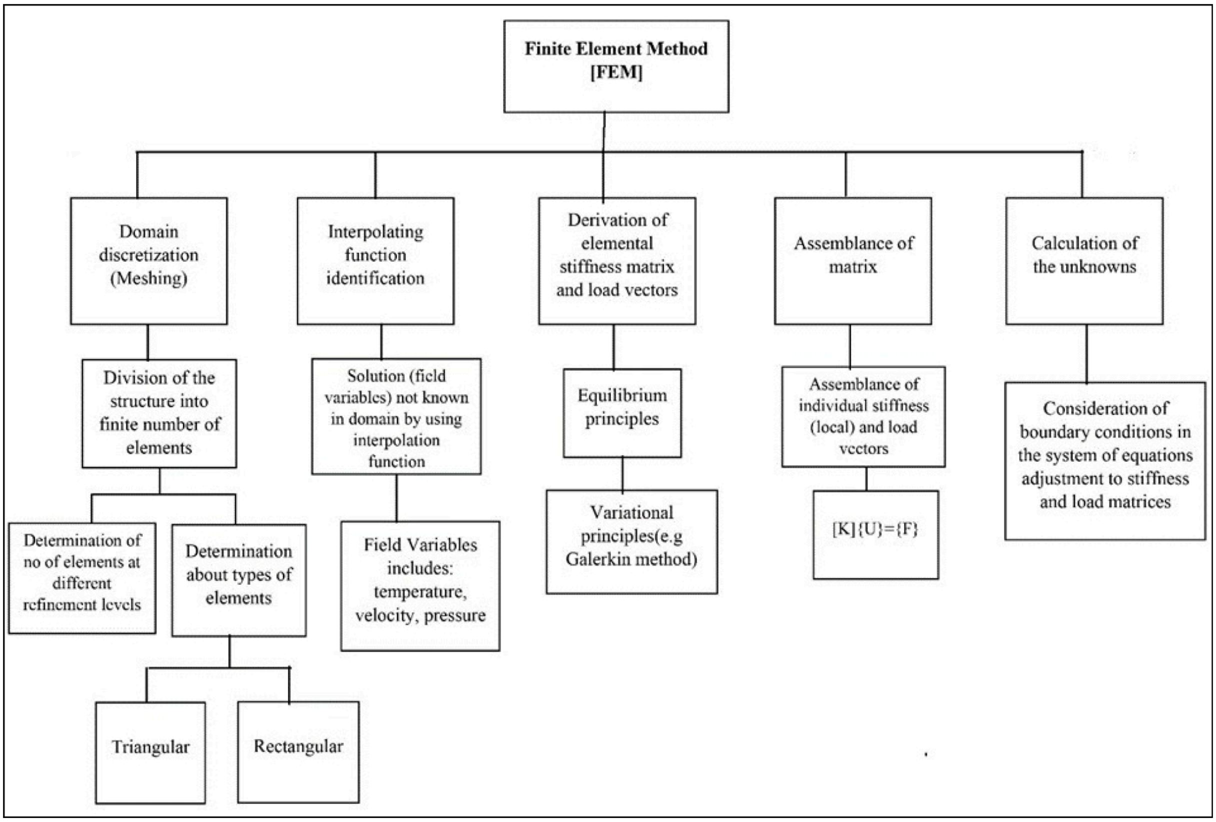

Fig. 3. Diagram representing steps involved in scheme.

$$\int_\Omega \left(U^* \frac{\partial V^*}{\partial X^*} + V^*.\frac{\partial V^*}{\partial Y^*} \right) w d\Omega + \int_\Omega \frac{\partial P^*}{\partial Y^*} w d\Omega + Pr \int_\Omega \left[\left(1 + \frac{1}{\beta} \right) \left(\frac{\partial V^*}{\partial X^*}. + \frac{\partial V^*}{\partial Y^*} \right) + \Lambda_{y^*} \right] w d\Omega = 0 \quad (28)$$

Integral form of mass conservation equation is described as under.

$$\int_\Omega \left(\frac{\partial U^*}{\partial X^*} + \frac{\partial V^*}{\partial Y} \right) q d\Omega = 0 \quad (29)$$

$$\int_\Omega \left(U^* \frac{\partial \theta^*}{\partial X^*} + V^* \frac{\partial \theta^*}{\partial Y^*} \right) w d\Omega - \int_\Omega \left(\frac{\partial^2 \theta^*}{\partial \theta^{*2}} + \frac{\partial^2 \theta^*}{\partial Y^{*2}} \right) w d\Omega = 0, \quad (30)$$

$$\int_\Omega \left(U^* \frac{\partial C^*}{\partial X^*} + V^* \frac{\partial C^*}{\partial Y^*} \right) w d\Omega - \frac{1}{Le} \int_\Omega \left(\frac{\partial^2 \theta^*}{\partial \theta^{*2}} + \frac{\partial^2 \theta^*}{\partial Y^{*2}} \right)$$

Continuous solutions is approximated by discrete ones in the finite dimensional sub-spaces.

$$U^* \approx U^*{}_h \in W_h V^* \approx V^*{}_h \in \quad (32)$$

$$\theta^* \approx \theta^*{}_h \in W_h$$

$$C^* \approx C^*{}_h \in W_h P^* \approx P^*{}_h \in Q_h$$

$$\int_\Omega \left(U^*{}_h \frac{\partial U^*{}_h}{\partial X^*} + v \frac{\partial U^*{}_h}{\partial Y^*} \right) w_h d\Omega + \int_\Omega \frac{\partial P^*{}_h}{\partial X^*} w_h d\Omega - Pr \int_\Omega \left(1 + \frac{1}{\beta} \right) \left(\frac{\partial^2 U^*{}_h}{\partial X^{*2}} + \frac{\partial^2 U^*{}_h}{\partial Y^{*2}} \right) w_h d\Omega + \Lambda_{X^*} \quad (33)$$

$$\int_\Omega \left(U^*{}_h \frac{\partial V^*{}_h}{\partial X^*} + V^*{}_h \frac{\partial V^*{}_h}{\partial Y^*} \right) w_h d\Omega + \int_\Omega \frac{\partial P^*{}_h}{\partial X^*} w_h d\Omega - Pr \int_\Omega \left(1 + \frac{1}{\beta} \right) \left(\frac{\partial^2 U^*{}_h}{\partial X^{*2}} + \frac{\partial^2 U^*{}_h}{\partial Y^{*2}} \right) w_h d\Omega + \Lambda_{Y^*} \quad (34)$$

$$\int_\Omega \left(\frac{\partial U^*{}_h}{\partial X^*} + \frac{\partial V^*{}_h}{\partial Y^*} \right) q d\Omega = 0, \quad (35)$$

$$\int_\Omega \left(U^*{}_h \frac{\partial \theta^*{}_h}{\partial X^*} + V^*{}_h \frac{\partial \theta^*{}_h}{\partial Y^*} \right) w_h d\Omega - \int_\Omega \left(\frac{\partial^2 \theta^*{}_h}{\partial X^{*2}} + \frac{\partial^2 \theta^*{}_h}{\partial Y^{*2}} \right) w_h d\Omega = 0, \quad (36)$$

$$\int_\Omega \left(U^*{}_h \frac{\partial C^*{}_h}{\partial X^*} + V^*{}_h \frac{\partial C^*{}_h}{\partial Y^*} \right) w_h d\Omega - \int_\Omega \left(\frac{\partial^2 C^*{}_h}{\partial X^{*2}} + \frac{\partial^2 C^*{}_h}{\partial Y^{*2}} \right) w_h d\Omega = 0, \quad (37)$$

In matrix representation.